EFFECT OF FORMULATION PARAMETERS AND PHYSIOLOGICAL ENVIRONMENT ON AMLODIPINE RELEASE KINETICS ENCAPSULATED IN BIODEGRADABLE POLYMERS AND OPTIMIZED BY DESIGN METHODOLOGY

Naima Ifourah,[1] **Sandrine Cammas-Marion,**[2] **and Hayet Belkacemi**[1,*]

In this study, two polyelectrolytes, chitosan and propyl methyl cellulose carbonate, were associated by crosslinking with tripolyphosphate (TPP), to prepare microspheres loaded with amlodipine besylate (Aml). The formulations were optimized by Box–Behnken experimental design, in which three factors, four responses were studied to check the effect of independent variables (concentration of TPP, pH of TPP solution, and pH of a polymer mixture) on responses: zeta potential, particle size, polydispersity index and entrapment efficiency. The optimal encapsulation efficiency was around 92.43%, the zeta potential on average 41.75 mV, and the minimum mean particle size was 310 nm. The effects of the parameters on changes in structure, crystallinity, and surface charges of polymers, by crosslinking in microparticles, were identified by FT-IR, XRD, and dynamic light scattering analyses. The encapsulation parameters and the environment media influenced the mechanism of release and the kinetics model, which was greater in the duodenal medium at pH 5.5 ($Q = 100\%$). The microencapsulation by nontoxic polymers in water is a good method of preparing amlodipine-loaded microspheres, which are intended for the oral route, with optimal dose release in the duodenal medium. This represents the target site for absorption of the drug, in the pulmonary sphere.

Key words: microencapsulation; chitosan; cellulose derivative; amlodipine; drug delivery.

INTRODUCTION

High blood pressure is a risk factor for mortality by cardiovascular disease. The majority of antihypertensive drugs that have been developed are in the form of oral tablets, 80% of which have low bioavailability and a hydrophobic nature [1]. Amlodipine (Aml) is a calcium antagonist belonging to the class of dihydropyridines [2]. After oral administration of Aml, its blood concentration is at its maximum between 6 and 12 hours, and most of the dose is linked to plasma proteins. A relatively high level of Aml is converted to inactive metabolites, resulting in low bioavailability [3].

In order to increase a drug's bioavailability (particularly Aml one), by avoiding the hepatic first-pass effect (high metabolism), as reported in work by Swamy and Abbas [4], a drug's microencapsulation may improve the therapeutic efficacy of the selected drug, and may constitute a promising approach. Indeed, such an approach may allow the vectorization of biologically active molecules by optimizing their physicochemical properties, such as solubility, and modifying their release kinetic profiles, leading to a site-specific and sustained release. The drug's encapsulation may also ensure, or at least improve, its protection against degradation into the gastrointestinal tract induced by the pH of the physiological medium and by the attack of epithelial or hepatic enzymes [5]. Sari, et al. [6] have shown that such strategy would make it possible to minimize unwanted effects by reducing the frequency of drug administration, and help to control the amount of drug released over time into the general circulation, while targeting the site of action.

Biocompatible and biodegradable, naturally available polymers, such as chitosan and cellulose derivatives, have attracted interest in the field of active substance encapsulation [7]. Solubilization of chitosan in an aqueous medium takes place by protonation of its primary amine (NH_2) groups

[1] Laboratory of Materials Technology and Process Engineering (LTMGP), Department of Process Engineering, Faculty of Technology, University of Bejaia, Algeria.
[2] Université de Rennes, Ecole Nationale Supérieure de Chimie de Rennes, CNRS, ISCR, UMR 6226, F-35000 Rennes, France.
[*] e-mail: hayet.belkacemi@univ-bejaia.dz

[8–10], forming positively charged aminium groups, thus leading to a cationic polyelectrolyte structure. Hydroxypropyl methylcellulose (HPMC) is a non-ionic semisynthetic polymer, whose solubility depends on the number of hydroxypropyl groups and is used to encapsulate bioactive molecules thanks to its swelling capacity [11, 12].

The chemical modification of HPMC was carried out in the presence of sodium carbonate, thus leading to carbonate of propyl methyl cellulose (CPMC) having an anionic polyelectrolyte structure. Association of the cationic chitosan with the anionic CPMC through the ionic crosslinking method leads to a more complex assembly formed by ionic interaction between the oppositely charged polyelectrolytes. This concept has already been studied by Cavallaro, et al. [13], in which the formation of a polyelectrolyte complex by the recombination of chitosan and alginate was demonstrated. In order to optimize the association between the two selected polymers (Chitosan and CPMC), sodium tripolyphosphate (TPP-Na) was used as a crosslinking agent, TPP-Na allows the strengthening links between the two antagonist polymers chains. To promote the stability of the chitosan/TPP/CPMC complex, cationic chitosan may interact with anionic CPMC through electrostatic forces forming bridges [14] with TPP, and resulting in a more stable three-dimensional network [15]. This ionic microencapsulation method has several advantages, i.e. it is a simple and inexpensive method [8], it avoids the use of toxic organic solvents, and it allows better encapsulation yield [16].

The response surface methodology has been widely adopted for the optimization of various formulation parameters of new drugs. The implementation of mathematical and statistical tools during the application of the experimental design are all major assets for the development, optimization, and improvement of new processes, in which a response of interest is influenced by several variables. Moreover, they define the effects of independent variables in combination and generate a mathematical model to analyze the responses as well [17]. This modeling is important for process optimization, because it provides essential information on the modes of interactions between the different factors and on the process response, while minimizing the number of tests [18]. In this context, our study was devoted to the optimization of the microencapsulation process of Aml in chitosan/CPMC-based microspheres. A Box–Behnken design with three factors, the quantity of TPP, the pH of the dispersed phase, and of the TPP solution, was implemented to show the influence of these factors on the main responses of the process. Important physicochemical characteristics of the obtained microcapsules, such as their surface charge (zeta potential), their mean size, and the rate of encapsulation, have been measured.

EXPERIMENTAL

Reagents

The hydroxy propyl methyl cellulose (HPMC) was supplied by SAIDAL-BIOTIC (Algeria) with a viscosity of 15 cps and a molar mass (Mw) of approximately 130,658 g/mol. Chitosan (Chit) (DD: 79.20%, Mw 68,001.82 g/mol) was supplied by "organic products" CAPBRETON (France) and was extracted from crab shells. The molecular weights of the polymers (HPMC, CPMC, Chit) were determined from the intrinsic viscosity, by applying the Mark–Houwink relationship. The method is based on measuring the flow time in the Ubbelohde capillary of aqueous solutions prepared under magnetic stirring for 2 h at 20°C, with different concentrations of polymers (0.05–0.4 g/dl). The DD of Chit was determined by conductometric titration of Chit solution in HCl 0.1 N, using NaOH solution at 0.1 N as titrant. Amlodipine besylate (Aml), an antihypertensive agent of the formula $(C_{20}H_{25}CIN_2O_5 \cdot C_6H_6O_3S)$ and molar mass of 567.1 g/mol, was supplied by SAIDAL-BIOTIC (Algeria). Sodium tripolyphosphate (TPP) and sodium carbonate Na_2CO_3 were supplied by PROLABO with an analytical grade of 99% purity. Milli-Q water was used for all studies in this work.

Methods

Chemical modification of HPMC

A quantity (50 g) of HPMC was dissolved in 250 mL of distilled water in a 500-mL beaker. This solution was transferred to a separating funnel placed over an Erlenmeyer flask, containing 250 mL of an aqueous solution of sodium carbonate (31.51 g). The HPMC solution was added dropwise into the sodium carbonate solution and maintained under continuous magnetic stirring at 25°C for 30 min. A white precipitate of milky appearance, related to the formation of the HPMC carbonate, was immediately formed after mixing the two solutions. Water was then evaporated under vacuum at 90°C for 24 h. After total water evaporation, the white precipitate was dried at 100°C for 24 h, and the weight (65 g) of the product (CPMC) was weighed with an accuracy of ±0.1 mg [19].

Preparation of microparticles

Microparticles of Chit/TPP/CPMC loaded with Aml were prepared by the ionic crosslinking method using sodium tripolyphosphate as a crosslinker. 1 mL of an ethanol solution containing 10 mg of Aml was added dropwise to a mixture of 5 mL of 2% acetic acid aqueous solution containing Chit at a concentration of 15 mg/mL (75 mg) and 5 mL of CPMC aqueous solution at a concentration of 20 mg/mL (100 mg), with strong magnetic stirring for 1 min. This mixture was added dropwise using a syringe into 100 mL of a TPP solution (at different concentrations) with moderate magnetic stirring (100 rpm), for 30 min. At the end, the sus-

pension was centrifuged twice at 6,000 rpm for 20 min. The microparticles were washed with 20 mL of distilled water, dried in the open air for a few days, weighed, and stored in PET pillboxes [20].

Encapsulation efficiency of Aml

The encapsulation efficiency was measured using UV analysis [21] of the supernatants of the microspheres' samples, at the maximum wavelength, l_{max}, of 366 nm of Aml. By comparing absorbance values of drug formulations with the standard curve, the specific concentration of the encapsulated active substance was calculated. Encapsulation efficiency (1) was calculated according to the formula given below:

$$\text{Encapsulation efficiency (\%)} =$$
$$= \frac{(\text{total drug} - \text{unencapsulated drug})}{\text{total drug}} \times 100, \qquad (1)$$

where *total drug* represents the concentration (mg/L) of Aml initially introduced before encapsulation and *unencapsulated drug* is the concentration (mg/L) of Aml after encapsulation in the supernatants after centrifugation.

Experimental design method

The Box–Behnken design, a type of response surface method adopted in pharmaceutical systems and particulate carriers, was selected. It provides detailed information on the interaction between various factors. A three-factor, three-level design was used to explore the quadratic response surfaces and construct second-order polynomial models, using Minitab and JMP7 programs [22]. In the present investigation, the amount of crosslinking agent TPP (X_1) and the pH of both solutions of TPP (X_2) and polymers (X_3) were selected as independent variables (Table 1); the 15 tests of the formulations are specified in the matrix in various runs, corresponding to the conditions of the three parameters, whereas the zeta potential, particle size, Polydispersity Index (PDI), and the encapsulation efficiency, were chosen as Y_1, Y_2, Y_3, and Y_4 responses respectively (Table 2).

TABLE 1. Variables used in the Box–Behnken experimental design

Factors	Levels		
	Low (−1)	Medium (0)	High (+1)
X_1: Amount of TPP (%)	0.25	1.125	2
X_2: pH of TPP solution	4	6	8
X_3: pH of polymer solution	4	5	6

Study of the release kinetics

Preparation of dissolution media

- Duodenal medium (pH 5.5): was prepared by mixing 12.04 g of sodium acetate dissolved beforehand in distilled water, with 6 mL of a 2-M acetic acid solution. The mixture was reduced to 2 L with distilled water.

- Intestinal medium (pH 6.8): a phosphate buffer solution was first prepared by dissolving 6.8 g of monopotassium phosphate in 250 mL of distilled water. This solution was mixed with 77 mL of 0.2 M NaOH solution. The resulting mixture was diluted to 1 L with distilled water.

- Blood medium (pH 7.4): a mixture of 8 g of NaCl, 0.76 g of di-sodium hydrogen phosphate (Na_2HPO_4), 0.2 g of potassium chloride (KCl), and 0.2 g of potassium dihydrogen phosphate (KH_2PO_4, was dissolved in distilled water and reduced to 1 L.

Dissolution test

A quantity (50 mg) of microspheres was introduced into a 1-L beaker, containing 900 mL of dissolution medium, and placed in a water bath at $37.0 \pm 0.1°C$, under continuous stirring with a paddle stirrer at 50 rpm. Samples of 3.5 mL were taken with a syringe at time intervals with a well-defined step from t = 0 min to $t = 270$ min. Each sample was filtered through a 0.45-µm microsyringe filter in a test tube. The filtered solutions were analyzed by UV–visible spectrophotometry, relative to the blank (physiological medium). The measured absorbances were compared with those of the calibration curves, for each dissolution medium, at the specific wavelengths of Aml, which were 369 nm, 366 nm, and 370 nm respectively, at pH 5.5, 6.8, and 7.4.

Microparticles characterization

Differential scanning calorimetry analysis

Thermograms of drug and prepared microparticles were performed using TA instruments model Q10. Ten milligrams of microspheres were put in an aluminum pan, and thermograms were obtained at a scanning rate of 10°C/min, within the temperature range 10°C to 200°C under a nitrogen atmosphere [21].

X-ray diffraction

Morphological analysis by x-ray diffraction (XRD) is a method used for determining the crystallographic structure of a crystal cell-constituting substance. In the present study, this method can give information on the crystallinity evolution of the polymers and of the active principle in the microparticles after encapsulation, under different process conditions, as well as the influence of the crosslinking reaction on the assembly of the two polyelectrolytes. The x-ray analysis was carried out on samples of microparticles, by comparison with the polymers and the starting active sub-

stance, using a Panalytical X-Pert PRO powder diffracto-meter model, by emission of $Cu(K_\alpha)$ radiation at room temperature, for a range of 2 theta between 5° and 60°, with a resolution of 0.04° and a scanning speed of 2°/min [23].

Scanning electron microscopy

The scanning electron microscopic (SEM) observations were carried out on the surface of Chi/CPMC/Aml micropar-ticle formulation using a TESCAN Microscope, with an electron beam energy of 15 kV.

Fourier transform infrared spectroscopy

Fourier transform infrared spectroscopy spectra were recorded at 4 cm^{-1} resolution within 40 scans, using a Nicolet IR-ATR IS5 spectrometer, within the range 4000 cm^{-1} to 500 cm^{-1}. These experiments were used to confirm the presence of Aml in the microparticles, the effect of the reticula-tion association between the two polymers and the crosslinking agent (TPP), and to elucidate the structure of the modified product (CPMC) with carbonate sodium [21].

Zeta potential, particle size, and Polydispersity Index measurement

Measurements of zeta potential are commonly used to predict the stability of colloidal systems and measure the surface charges of particles. These characteristics are highly sensitive to pH and ionic strength. In this study, zeta potentials of Chit–CPMC nano- or microparticles crosslinked by TPP, were measured in distilled water by electrophoretic light scattering (ELS) using a Nano-sizer ZS90 (Malvern) at 25°C, with a He-Ne laser at 633 nm and a detection angle of 90°C. The measurements were repeated at least three times and the results were given as the mean values of the zeta potential of microparticles relative to the starting polymers. Particle size and dispersity are among the most important characteristics of particulate systems that are measured by the same apparatus. Dry microspheres (5 mg) were suspended in distilled water and ultra-sonicated for 5 min. For each sample, the measurement was repeated three times, and the average of the three measurements was calculated. A drop of suspension was placed on a clean glass slide, and the microspheres were counted under an optical microscope [24]. The data processing software associated with this device also gives access to a value denoted as the PDI, which provides information on the size dispersion of the particles in the sample, as well as on the presence or absence of aggregates. The closer the PDI value is to 1, the sample is said to be polydisperse. Conversely, when the PDI is small the sample is said to be monodispersed and the sample will be of more homogeneous size.

TABLE 2. Box–Behnken experimental design in various runs and obtained responses

Formulation	Independent factors			Responses			
	X_1	X_2	X_3	Zeta Potential (Y_1) (mV) (*mean ± SD)	Size (Y_2) (nm) (*mean ± SD)	PDI (Y_3) (*mean ± SD)	Encapsulation efficiency (Y_4) (%) (*mean ± SD)
FMP1	0.250	4	5	49.04 ± 1.01	490 ± 39.3	0.227 ± 0.040	90.49 ± 0.58
FMP2	0.250	8	5	51.25 ± 0.82	1481 ± 66.6	0.293 ± 0.008	90.59 ± 1.23
FMP3	2.000	4	5	41.75 ± 0.93	310 ± 45.2	0.201 ± 0.008	92.43 ± 1.70
FMP4	2.000	8	5	51.50 ± 0.93	1844 ± 112.4	0.280 ± 0.040	91.41 ± 5.74
FMP5	1,125	4	4	47.35 ± 2.21	411 ± 8.4	0.215 ± 0.003	90.76 ± 6.35
FMP6	1.125	4	6	43.25 ± 1.08	401 ± 27.7	0.224 ± 0.003	89.75 ± 1.76
FMP7	1.125	8	4	52.00 ± 1.32	759 ± 16.8	0.345 ± 0.030	89.29 ± 0.20
FMP8	1.125	8	6	48.50 ± 2.50	2400 ± 100	0.370 ± 0.030	90.67 ± 0.20
FMP9	0.250	6	4	53.00 ± 2.25	430 ± 5.7	0.263 ± 0.010	88.73 ± 3.39
FMP10	2.000	6	4	47.00 ± 2.19	455 ± 10.9	0.203 ± 0.037	88.18 ± 3.00
FMP11	0.250	6	6	49.00 ± 2.53	1059 ± 100.1	0.389 ± 0.037	87.53 ± 4.77
FMP12	2.000	6	6	48.00 ± 0.93	1390 ± 79.4	0.219 ± 0.010	92.15 ± 5.02
FMP13	1.125	6	5	48.50 ± 1.88	700 ± 164.1	0.171 ± 0.001	91.51 ± 0.13
FMP14	1.125	6	5	48.50 ± 1.70	845 ± 27.9	0.170 ± 0.000	91.69 ± 5.47
FMP15	1.125	6	5	48.00 ± 0.50	701 ± 35.3	0.169 ± 0.001	91.32 ± 0.13

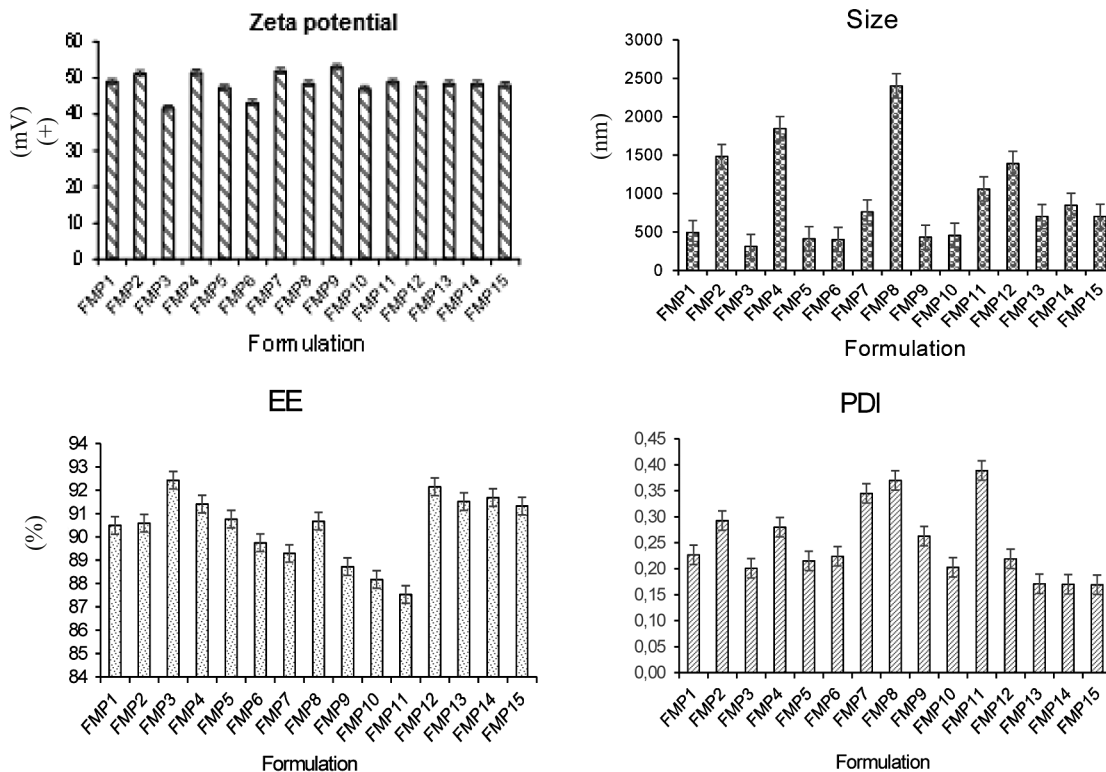All the values are expressed as mean ± SD, SD: Standard deviation, where * $n = 3$.

Fig. 1. Histogram of responses by the Box–Behnken design of Chit/TPP/CPMC microspheres loaded with amlodipine and prepared by ionic crosslinking.

RESULTS AND DISCUSSION

Design method

The problem was based on three factors: the concentration of the TPP (crosslinking agent), the pH of the TPP solution, and the pH of the two-polymer mixture. Indeed, results have shown (Fig. 1) that these factors have more or less significant effects on the four main responses measured (Table 2): the zeta potential, the size of the particles, the PDI, and the encapsulation efficiency of the active drug. It is noted that the values of SD vary from one formulation to another; for the response of the potential zeta the highest value (±2.53) is obtained for the formulation of FMP11 whereas the lowest value (±0.50) is obtained for the FMP15 test. This shows that the measurements deviate much less from the average when the formulation is prepared under the average conditions of the factors used for encapsulation. Furthermore, the lower value of SD (±5.7) for the particle size corresponds to the FMP9 formulation prepared with less TPP and at a higher pH (8) but for an acidic pH (4) of the polymer solution. The lowest value of the standard error (±0.001–0.000) relative to the PDI was obtained for the three central trials (000) of the FMP13, FMP14, and FMP15 formulations, with the lowest values of PDI (0.171–0.169). It should also be noted that the highest encapsulation rate (92.43%) was ob-

tained for the FMP3 formulation, characterized by a smaller size of microparticles (310 nm) and the lowest zeta potential (+41.75 mV) with a relatively low PDI (0.201).

This shows that the use of a smaller amount of TPP, so that the crosslinking of the two polymers is less favorable, decreases the size of the particles to give a sample of microspheres of more homogeneous sizes. On the other hand, the two formulations FMP13 and FMP15 give encapsulation efficiency values closer to the average, with the same minimum SD deviation value (±0.13). This proves that under the average conditions of the encapsulation factors (central points) the measurements of the encapsulation efficiency are more precise. The electrostatic interactions between the positively charged Chit chains (protonated NH_3^+) and the modified negatively charged CPMC polymer (rich in carbonate groups CO_3^{2-}) in the presence of the crosslinking agent (TPP), have led to the formation of hydrogen bridges between two pairs of polymer chains (Chit/CPMC). Such interactions allowed a better stabilization of the Chit/CPMC/TPP assembly, favored by the lowering of the steric constraints that may exist between the associated chains. This allows the strengthening of the three-dimensional network, in accordance with the work of Li and Lin [15], who showed that this crosslinking formed a more stable structure at pH 6.
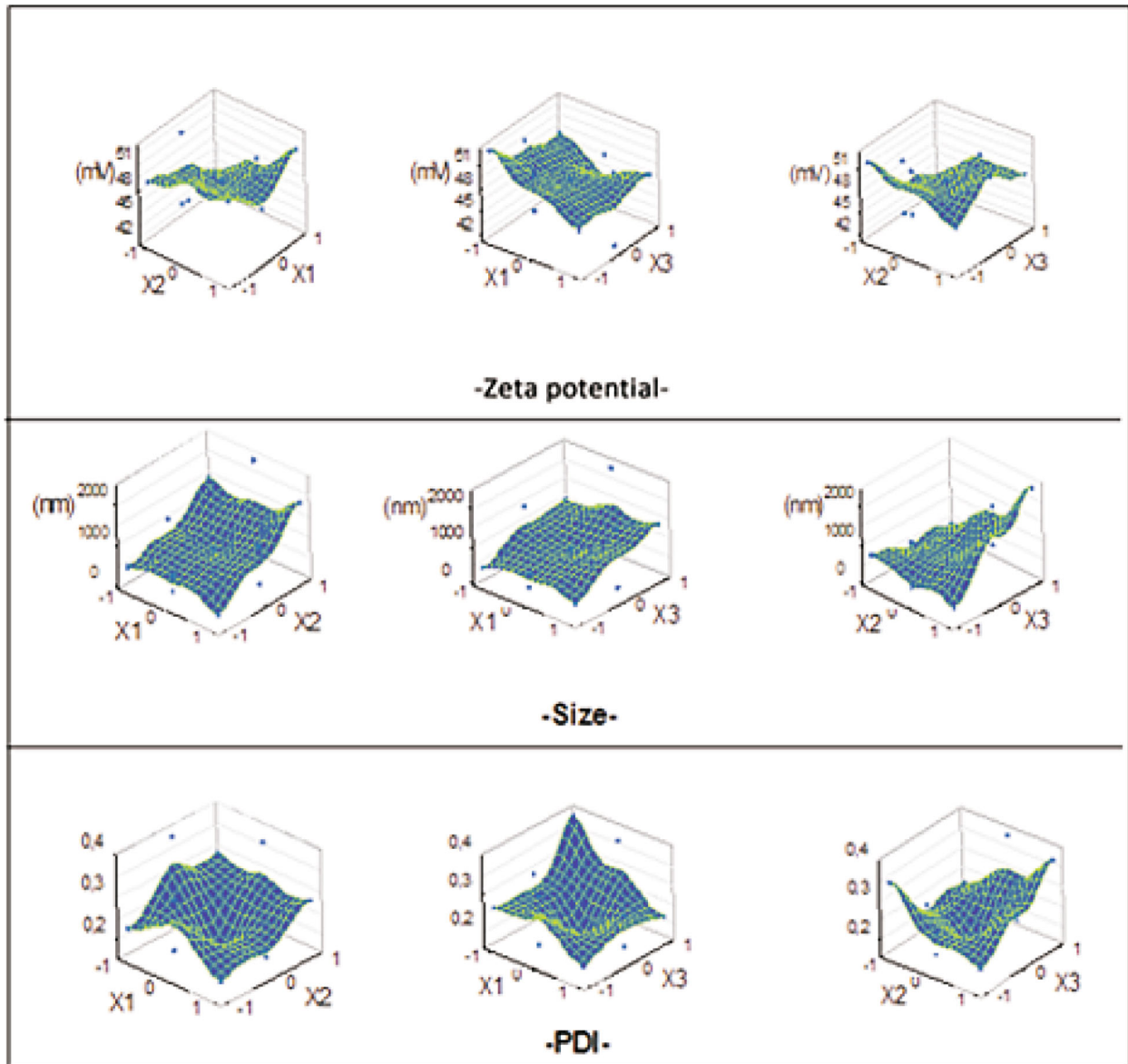
Fig. 2. Response surface of the zeta potential, size, and PDI of microparticles as a function of TPP amount (X_1), pH of TPP solution (X_2), and pH of polymer solutions (X_3).

This decisive factor can significantly affect the physicochemical properties of the Aml-loaded microparticles, as well as the release profile of the active principle in the various physiological media. Therefore, to optimize the encapsulation process of Aml, we must select the main factors related to TPP and polymers.

Effect of factors design on microparticles properties

Zeta potential, size, and PDI are the most important physicochemical properties of micro- or nanoparticles, which were influenced strongly by the parameters of design in the formulation of Chit/CPMC microspheres loaded with amlodipine. The stability of colloidal systems is directly re-

lated to their surface charges represented by the zeta potential values. Such values provide information on the stability of the colloidal systems: when the zeta potential values are either lower than or equal to –30 mV or higher than or equal to +30 mV, the corresponding formulation is known to be electrostatically stable. Moreover, the surface charges of such colloidal systems define the adhesion or not of biomolecules such as opsonins, the adhesion or not onto biological surfaces, and the nonspecific uptake by the liver and or spleen [25].

In Fig. 2, the surface of the zeta potential (Y_1) of the microparticles and the influence of the factors on this response were represented. If we considered only the two vari-

ables (X_1, X_2), the response surface design showed that the zeta potential increased when the amount of TPP (0.25–2%) and the pH of TPP solution (4–8) increased between the maximum and minimum values.

However, this parameter was less influenced by the second variable X_2, and the highest value (+53.00 mV) was obtained for the lower value of X_1 = 0.25 and the central value of X_2 = 6. The values decreased when the quantity of TPP (X_1) increased from 0.25% to 2%, and increased between 4 and 6 with the pH of polymer solution (X_3). Such behavior may be the result of the decrease in the number of NH_3^+ groups and the degree of ionization of Chit. The results revealed a low overall positive charge density and zeta potential of the microparticles, on which the solubility of the biopolymer depends. Conversely, the zeta potential increased when the two variables (X_2, X_3) exerted an effect at the same time on the response, when the pH of the TPP increased to 8 and that of the polymer solution decreased to 4. As the property of surface charges is known to be very sensitive to pH and ionic strength, it highlights the importance of electrostatic forces acting between different particles of opposite charges, as described by Joye and McClements [26]. In addition, recent work has shown that the zeta potential values are affected by the interaction between the two polyelectrolytes, and with the TPP, and were essentially influenced by two parameters, the ionic strength and the pH of the Chit solution [27].

In our study, it is important to note that measured zeta potential values for all 15 formulations were within the range +42 to +53 mV, values clearly higher than those obtained for CPMC (−16.5 mV) and HPMC (−6.33 mV). Such results highlighted that the surface of the microparticles was positively charged, owing to the predominance of Chit chains at the surface of the prepared microspheres. The protonated NH_3^+ amino groups were thus oriented toward the surface, whereas the negatively charged CPMC chains were oriented toward the inner core of the prepared microspheres.

The particle size values, reported in Table 1, were largely influenced by the independent variables (Fig. 2), and were within the range between 310 nm and 2400 nm. Particle size is one of the most important parameters that determines the biocompatibilities and bioactivities of micro- and nanoparticles, the latter having greater intracellular absorption than the former. Desai and Park [28] reported that the gastrointestinal absorption of particles with a size of 100 nm was 15 to 250 times greater than that of larger microparticles.

By increasing the values of the variables (X_1, X_2, X_3), we noticed an increase in the mean particle sizes, which reached a maximum value of 2400 nm (Fig. 2). On the contrary, their decrease induced a decrease in the value of the response Y_2 to the minimum value of 310 nm. This was favored by the decrease in the degree of protonation of the amine groups of chitosan [29], which minimized the interactions induced by electrostatic repulsion forces, between the chains of the polymer and ionic species of the crosslinking agent (TPP).

Correlatively, it should be noted that the PDI value decreases with the size of the nanoparticles (Fig. 1), as in the case of the FMP3, FMP13, FMP14, and FMP15 formulations prepared in a continuous phase (polymer solution) at a pH of 5, where the Chit is more soluble. The smaller a particle, the more its Brownian motion increases, and the more the populations of nanoparticles are homogeneous, with similar dimensions and tend toward the same average diameter. The standard deviation (SD) on the mean value of the PDI is the lowest, estimated at 0 and 0.001 (Table 2), for the formulations corresponding to the central point (000). Furthermore, the lowest PDI values are obtained for the formulations (Fig. 2) corresponding to the average pH values of the TPP solution (X_2 = 6 or 0 in coded value) and of the polymer solution (X_3 = 5 or 0 in coded value), while for the value of the TPP rate is the highest (X_1 = 2% or 1 in coded value), owing to the higher ionic strength of the solution [30].

Effect of factor design on the encapsulation efficiency of Aml

The encapsulation efficiency is defined as the difference between the initial concentration added for the formulation preparation and the concentration loaded into the formulation. Aml encapsulation values in Chit/CPMC microspheres were within the range 87.53 to 92.43%. At the same time, the representations (Fig. 3) of the surface response encapsulation efficiency (%) showed that the effect of the three variables on the encapsulation efficiency was not the same as on the size as well as on zeta potential of microparticles. Optimal values of the encapsulation efficiency were obtained at X_1 = 2% and X_2 = 4. On the other hand, two maximums, one at X_2 = 6 and X_3 = 5 and the other at X_2 = 4 and X_3 = 5, were observed.

Correlatively, it was noted that the value of X_1 = 2% was associated with the value of X_3 = 5, resulting in the best encapsulation efficiency of 91.41% for the formulation FMP4. This confirmed that the best pH of the solution polymers could be a value of 5. On the other hand, the amount of TPP appeared to be optimal at 2%. Correlative to these results, it appeared that a TPP solution pH of 4 positively influenced the encapsulation efficiency, which reached the optimal value of 92.43% for assay 3 (FMP3). We have shown that when the amount of TPP increased, the surface charges of the microparticles decreased. This effect might be explained by the negative charge of the phosphate ions, which partially compensates for those of the protonated amine groups formed in an acidic medium. This inevitably led to a decrease in the overall positive surface charge [31].

The result was comparable with those obtained in the study [29] carried out on the encapsulation of vitamin C in a Chit/TPP matrix, which showed that the elevation of TPP content resulted in a decrease in the zeta potential for the microparticles. The phenomenon was linked to the degree of ionization of the TPP, which depended on the pH of the medium. In a basic medium, the predominance of the phosphate
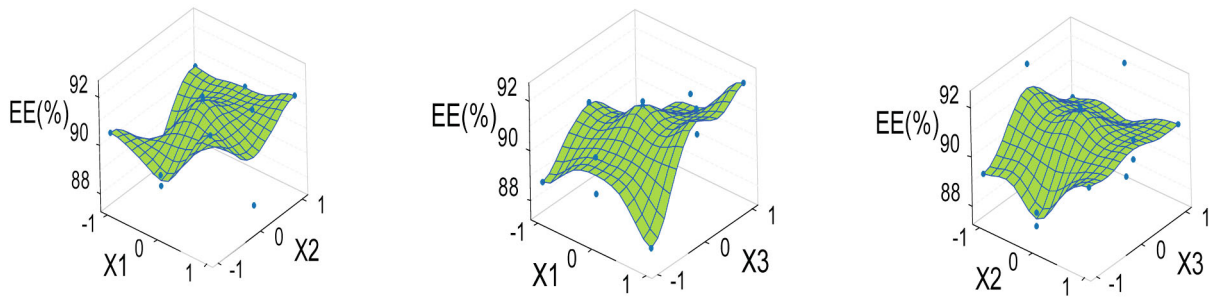
Fig. 3. Response surface of encapsulation efficiency (%) as a function of TPP amount (%) (X_1), pH of TPP solution (X_2), and pH of the polymer solution.

ions PO_4^{3-} was favored by dissociation of the TPP, which precipitated in solution at pH 8. This led to a decrease in the interactions of the TPP ions with the Chit chains and the degree of crosslinking of the corresponding microparticles. This further promoted the dissociation of protonated amine groups existing on the surface of the microparticles, by increasing the surface charge of the microparticles to the maximum value of +53 mV.

On the other hand, in the case of an acidic solution of TPP at pH 4, we noticed the predominance of phosphoric ions ($P_3O_{10}^{5-}$) of the TPP, which diffused more easily between the chains of Chit by Coulomb attractive forces, induced by the (NH_3^+) groups of Chit. Their positive charges were partially offset by anions ($P_3O_{10}^{5-}$), which decreased the overall value of the zeta potential to +41.75 mV, and increased the degree of crosslinking of Chit in an acidic medium [32, 33]. It has been shown that increasing the concentration of the crosslinking agent causes a slight increase in particle size. This result was attributed to the existence of inter- and intramolecular crosslinks, which resulted in the formation of aggregates and an increase in particle size [34], owing to a strong association of Chit chains at a weakly basic pH. This parameter strongly depends on the pH of the crosslinking medium, and consequently on the pH of the TPP solution [35]. In fact, at pH greater than 6, the overall positive charge of Chit decreased appreciably by deprotonation of the amino groups. This resulted, on the one hand, in the reduction of electrostatic interactions between the different charged groups and, on the other hand, in the solubility of the polymer in water [36]. The increase in the concentration of the crosslinking agent has led to an increase in the encapsulation efficiency. A similar result was already obtained in the study on the encapsulation of felodipine in the microparticles of Chit associated with tripolyphosphate, prepared using the ionic crosslinking method, according to the work of Desai and Park [28]. The higher the amount of crosslinking agent, the more it promoted the crosslinking reaction, and in this case the formation of free-flowing microspheres, with a marked increase in the level of encapsulation of Aml [37].

Validation of response models

The factors and model terms that significantly affected the zeta potential of Aml-loaded microparticles, and that showed highly significant effects on the Y_1 response (zeta potential), were those whose probabilities were within the confidence interval of 95% minimum, with a probability that the real value deviates the most from the theoretical or ideal value $p \leq 0.05$. The terms that most influenced the Y_1 response (zeta potential) were in decreasing order, X_1 (quantity of TPP) of probability $p = 0.0018$, followed by X_2 (pH of the TPP solution) corresponding to $p = 0.0002$, and then X_3 (pH of the solution of polymers) of $p = 0.0059$. The terms of the interactions at order 2 also significantly influenced the response, such as X_1X_2 with a probability of $p = 0.0058$ and X_1X_3 of probability $p = 0.0282$. However, the most significant parameter was the pH of the TPP solution corresponding to the lowest probability. On the other hand, the other terms, such as the quadric effect of the quantity of TPP (X_1^2, $p = 0.1328$), of the pH of the TPP solution (X_2^2, $p = 0.1553$) and the pH of the solution of the polymers corresponding to the dispersed phase (X_3^2, $p = 0.7333$), did not significantly influence the values of the zeta potential (response Y_1). Given that their probabilities greatly exceeded the limit value ($p > 0.05$), the values of the Y_1 response will be outside the confidence interval of the response predicted by the model. The effect of these three parameters on the zeta potential was described by the following model equation (2):

$$Y_1 = 48.33 - 1.755X_1 + 2.7325X_2 - 1.325X_3 +$$
$$+ 0.763X_1^2 - 0.712X_2^2 + 0.156X_3^2 + 1.885X_1X_2 + \quad (2)$$
$$+ 1.250X_1X_3 + 0.150X_2X_3.$$

The positive value in the regression equation showed the effect that favored the response (synergistic effect). On the other hand, the negative value indicated that the effect was against the response (antagonistic effect). By examining the equation of the Y_1 response, it clearly appeared that the model coefficients verified that the amount of TPP (X_1) and
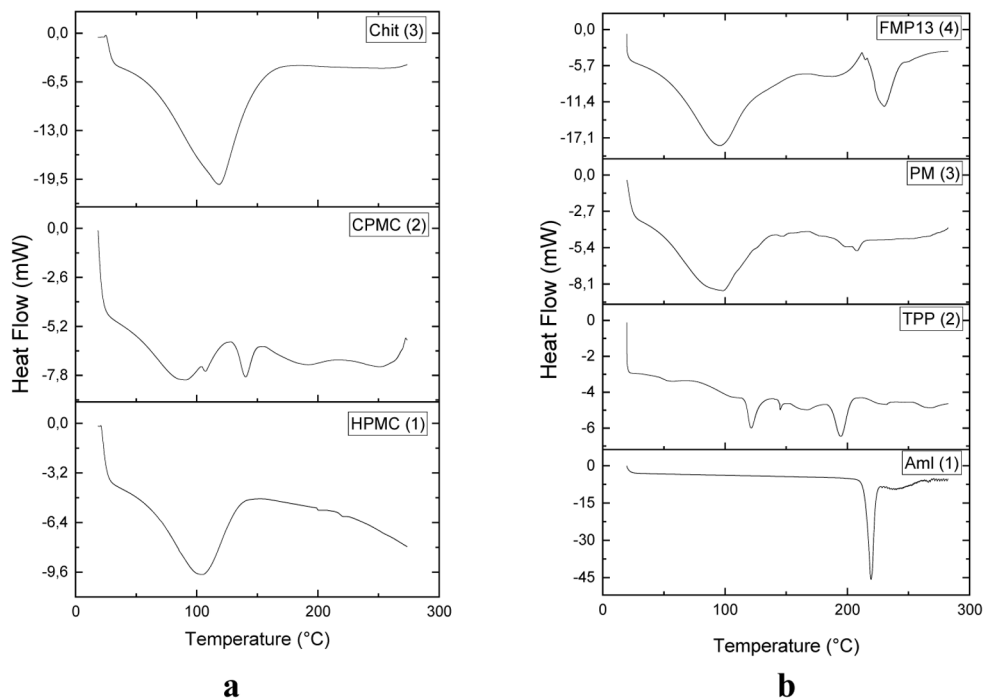
Fig. 4. DSC thermograms of: a) 1 – HPMC, 2 – CPMC, 3 – Chitosan; b) 1 – Amlodipine besylate, 2 – TPP, 3 – microparticles of physical mixture formulation (PM), 4 – microparticles of FMP13 drug formulation.

the pH of the dispersed phase (X_3) had negative effects, whereas the pH of TPP had a positive effect on the zeta potential. The coefficient of determination of this model was $R^2 = 0.97$, and the value of the adjusted coefficient of determination was $R^2ajus = 0.92$. The obtained results confirmed that the real values were quite close to the predicted ones.

The results obtained by the mathematical model showed that the influence of the three parameters studied on the response of the average particle size (Y_2) had a very significant effect for the three factors. Indeed, the probability of X_1 (amount of TPP) was $p = 0.034$, although it was very low ($p < 0.0001$) for X_2 (pH of the TPP solution) and X_3 (pH of the polymer solution). These last two factors best predicted the Y_2 response. Moreover, according to the equation of the model of Y_2, it can be seen that all the terms up to order 2 in interactions and in the second degree had a positive influence (synergistic effect) on particle size. The coefficients of the terms were quite high, in particular for the factor X_2 (522), and for the interaction term X_2X_3 of order 2 with a relatively high coefficient (586.7), as well as that of X_3 of no less negligible coefficient (399.4). This shows that the effect of these parameters favored the increase in particle size. The most significant parameters were the pH of the TPP (X_2) as well as the pH of the dispersed phase (X_3) and the interaction term X_2X_3 with the same probability ($p < 0.0001$). On the other hand, the interaction term X_1X_2 ($p = 0.0096$) was less significant and had a probability less than 0.05, whereas the effect of the interaction of terms X_1X_3 ($p = 0.0700$ .1), which exceeded 0.05, was not included in the confidence interval

($^395\%$), indicating that this term had a nonsignificant effect. The equation (3) of the model of the particle mean size was as follows:

$$Y_2 = 748.7 + 67.4X_1 + 522.0X_2 + 399.4X_3 +$$
$$+ 61.7X_1^2 + 220.9X_2^2 + 23.2X_2^2 + 135.8X_1X_2 + \qquad (3)$$
$$+ 76.5X_1X_3 + 586.7X_2X_3.$$

The analysis of variance showed that the model was significant through the p value and the Fisher F index. In our study, the p value given by the model was less than 0.0001 and the value of F was very high, estimated at 131.6. The values of the coefficients of determination (R^2) and adjusted were 0.99 and 0.98 respectively, which indicated that the adjustment was optimal and of very good quality. ANOVA of the Y_3 (PDI) response, whose model equation (4) is expressed as follows:

$$Y_3 = 0.1700 - 0.0336X_1 + 0.0201X_2 + 0.0220X_3 +$$
$$+ 0.0301X_1^2 + 0.0501X_2^2 + 0.0684X_3^2 + 0.0033X_1X^2 - \qquad (4)$$
$$- 0.0275X_1X^3 + 0.0690X_2X^3.$$

This gave very significant quadratic terms ($p = 0.049 < 0.05$, $F = 10.66$), and X_3^2 is the most significant ($p = 0.022$; F value = 11.76) of the three quadratic terms. Nevertheless, the term that most significantly influences PDI and best predicts the model is the interaction term X_2X_3

($p = 0.019 < 0.0$; F value = 11.76). The coefficient of determination of this model was equal to $R^2 = 88.88\%$, for the three chosen parameters and their ranges of variations.

The negative coefficient terms (X_1 and $X_1 X_3$) act on the response by reducing the value of PDI. This shows that the more the values of the concentration of TPP and the pH of the solution of the polymers (Chit and CPMC) increase, the more the PDI decreases, the more the nanoparticles are dispersed and form the fewest aggregates. This is in agreement with the results for the size of the nanoparticles, where the parameters influence the Y_2 response in the same way.

The statistical study carried out by the program JMP7 of the Y_4 response (Aml encapsulation efficiency) was expressed by the following equation (5):

$$Y_4 = 91.507 + 0.854 X_1 - 0.185 X_2 + 0.392 X_3 -$$
$$- 0.362 X_1^2 + 0.347 X_2^2 - 1.736 X_3^2 - 0.280 X_1 X_2 + . \quad (5)$$
$$+ 1.293 X_1 X_3 + 0.597 X_2 X_3$$

and showed that the parameters that have significant effects in a 95% confidence interval ($\alpha = 0.1$) on the Y_3 response, were X_1 ($p = 0.0031 < 0.1$) and X_3 ($p = 0.057 < 0.1$). Other terms, such as the interactions $X_1 X_3$ ($p = 0.0023 < 0.1$), $X_2 X_3$ ($p = 0.0457 < 0.1$), as well as the quadratic terms X_1^2 ($p = 0.0453 < 0.1$), X_3^2 ($p = 0.0007 < 0.1$) also have very significant effects. On the other hand, X_2 ($p = 0.302 > 0.1$), the interaction of the terms $X_1 X_2$ and the quadratic interaction X_2^2 did not have a significant effect on the Y_4 response. The coefficient of determination of this model was $R^2 = 0.97$, and the fitted value was 0.90. The obtained results showed that the influence of the three main factors made it less possible to predict the response of the encapsulation efficiency (Y_4). However, the actual values were sufficiently close to the predicted ones and the ANOVA showed that the model was significant through the p value and the coefficient F estimated at 0.004 and 15.67 respectively. The optimized value predicted by the model, for encapsulation efficiency (Y_4), was estimated at 91.51% with an error of ±0.67%. The factor and the term that most influenced both the zeta responses (Y_1) and the particle size (Y_2) was X_2, with positive orthogonal estimated values of about 2 and 445 respectively. The effect of this term on the mean particle size (Y_2) was the largest, whereas the encapsulation response (Y_4) was more negatively influenced (-0.9) by the quadratic interaction term X_3^2, which depended on the pH parameter of the polymer solution.

Characterization of microparticles and polymers

Differential scanning calorimetric analysis

Chitosan and HPMC exhibited endothermic peaks, at 116.34°C and 93.38°C respectively (Fig. 4a), attributed to the evaporation of residual water trapped in the amorphous structure of these two hydrophilic polymers [38].
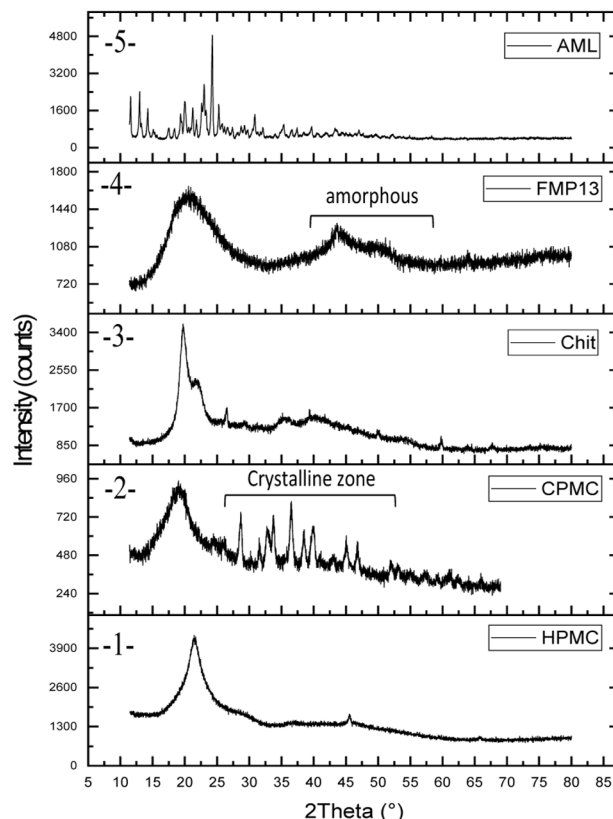

Fig. 5. Diffractograms X of: 1 – HPMC, 2 – CPMC, 3 – Chitosan, 4 – Microparticles of FMP13 formulation, 5 – Aml.

Furthermore, the microparticles containing Aml (Fig. 4b), entrapped either by encapsulation (Fig. 4, b-4) or by physical mixing (Fig. 4, b-3), exhibited an endothermic peak of Aml (Fig. 4, b-1) around 207°C in crystalline form of relatively greater intensity for the optimized formulation FMP13 (Fig. 4, b-4). Thereby, Aml was present at a higher concentration in the FMP13 formulation than in the physical mixture. Therefore, the interactions between molecules of the active principle on the one hand, and the functional groups of the polymer as well as of the TPP (Fig. 4, b-2) on the other, were greater when the Aml was entrapped by encapsulation than by physical mixing [39]. In addition to this peak, we noted an increase in the intensity of the endothermic peak at 230°C, due to a greater crosslinking process between the chains of the two polymers and the crosslinking agent [40]. At the same time, we observed the very marked decrease in the endothermic peak of Aml at 207°C and of the Chit peak shifted at a lower temperature (<100°C), which showed that molecules of the active principle were very dispersed in the microspheres of Chit/CPMC in the amorphous state [41].

X-ray diffusion analysis

Chemical modification of HPMC by carbonation has led to CPMC having a higher degree of crystallinity, thus leading
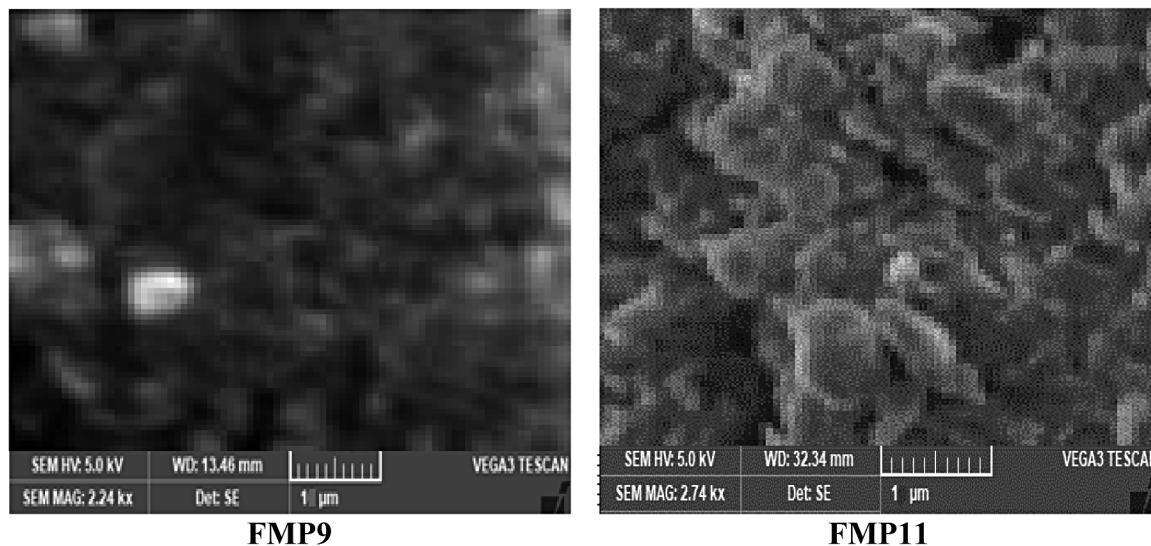
FMP9   **FMP11**

Fig. 6. Images by SEM of the microparticles with a high magnification (×50,000) of FMP9 and FMP11 formulations of Chit/CPMC/Aml microparticles.

to the appearance of new diffraction peaks at $2\theta = 19.06°$; $23.13°$; $28.75°$; and $33.75°$ (Fig. 5 – 2), unlike the x-ray diffractogram of HPMC, which showed practically only one peak at $2\theta = 20°$ (Fig. 5 – 1).

The x-ray diffractogram of chitosan showed two characteristic peaks at 2θ: $19.71°$ and $23°$, which are relatively intense, in addition to three other peaks of lower intensities at about $2\theta = 26°$, $35°$, and $45°$ corresponding to a semi-crystalline structure (Fig. 5 – 3). In conclusion, HPMC and chitosan were characterized by a semi-crystalline structure, whereas CPMC differed from the previous polymers by its more crystallized structure, in particular in the zones containing the carbonate substituents, in position C2' of the propyl radical. We noticed the absence of diffraction peaks of the microspheres loaded (Fig. 5 – 4) with Aml (Fig. 5 – 5), which showed that not only the degree of crystallinity of the active substance was reduced after the encapsulation process by the crosslinking method but also that the drug was highly dispersed in the amorphous matrix of the polymer [42].

SEM analysis

Observation by SEM of the microparticles of FMP9 and FMP11 gave the images in Fig. 6, which shows the existence of different shapes and sizes dependent on the conditions of microencapsulation preparation. For the FMP11 formulation, the shape of the microparticles is ovoid with a large size, but for the FMP9 formulation the shape is more spherical with a smaller size.

These observations correlate with the results given by zetametry and ELS measurements, which resulted in mean particle size values of 430 nm and 1059 nm for the FMP9 and FMP13 formulations respectively (Table 2).

The reduction in size in the case of the FMP9 microparticles is due to the pH of the solution of the polymers, which is more acidic (pH 4), favoring the protonation of the amine groups of the chitosan much more. The excess positive charge on the surface of the polymer chains clearly accentuates the electrostatic repulsions between the chains of the polymer and thus decreases the thickness of the layer of the microspheres. In addition, the basic pH (pH 8) of the TPP solution has the effect of pushing the negatively charged CPMC chains back as much as possible. This reduces the number of polymer chains that can associate with those of chitosan through the TPP.

FT-IR analysis

The infrared spectra of Aml, chitosan/CPMC/TPP microparticles of FMP13 and microparticles without active principle were shown in Fig. 7, and compared with FT-IR spectra of polymers, Chit, CPMC, and TPP. For the Chit, two characteristic bands of chitosan at 1650 cm^{-1} and 1588 cm^{-1}, were shown corresponding to $C = O$ (elongation) of the amide function (amide band I), and to NH_2 (deformation) of the amine function [14].

For the CPMC, we noted the disappearance of the band at about 1650 cm^{-1} of deformation of the OH bond in position C2' on the propyl radical, highlighting the substitution of carbonate $-OCO_2-$ on the propyl radical. On the other hand, new bands were observed at about 1267 cm^{-1} and 1146 cm^{-1} (medium to weak) attributed to the carbonate group (elongation), owing to the substitution of the CO bond on the propyl radical, and that of the $-(O-CO_2-)$ group of the carbonate respectively.

The appearance of three bands (medium to weak) at about 879 cm^{-1}, 805 cm^{-1}, and 711 cm^{-1}, very characteristic
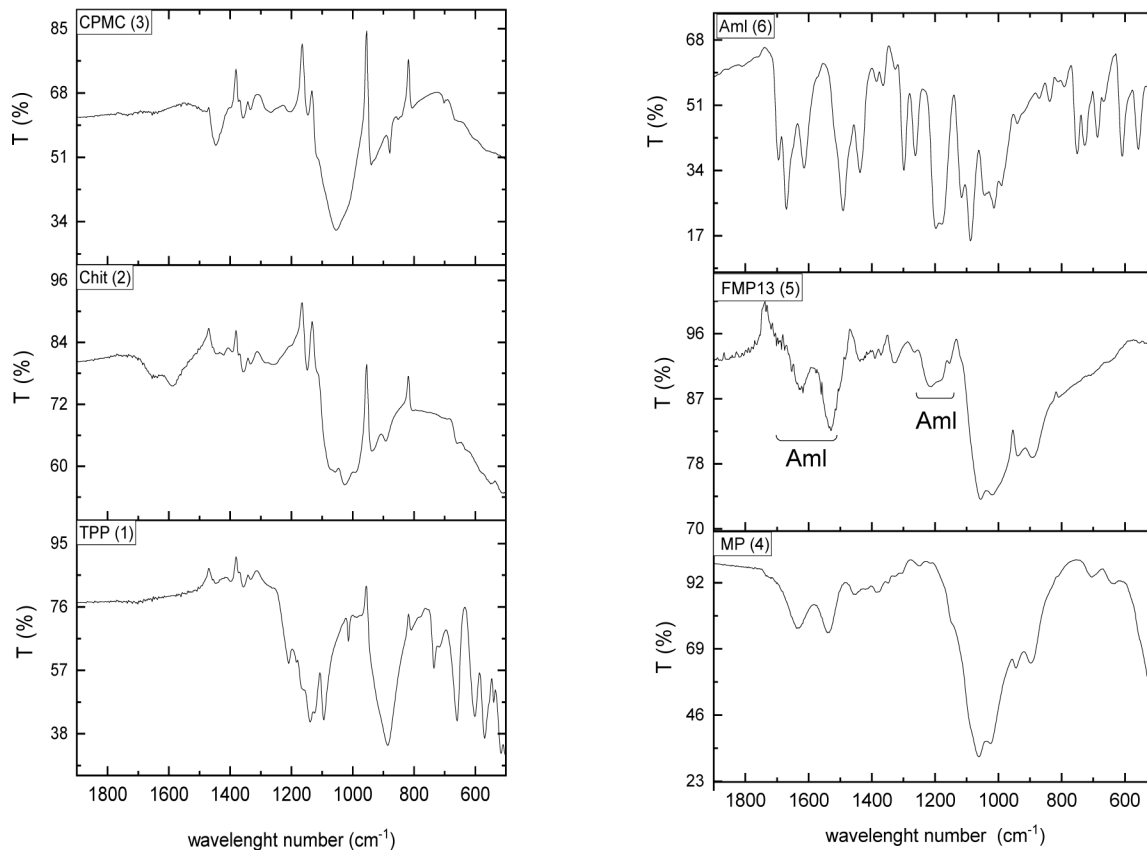
Fig. 7. Infrared spectra of: 1 – TPP; 2 – Chitosan; 3 – CPMC; 4 – microparticles without active drug; 5 – FMP13 formulation loaded with Aml; 6 – Aml.

of the carbonate grafted in C2', were respectively attributed to the bound OH (deformation) of the hydroxylated form (H-O-CO_2-), and to the superposition of the two bands of vibration of single valence $\upsilon2$ and degeneration $\upsilon4$ of (-OCO_2-) (Fig. 7 – 3). In addition, we noticed that the band at 1383 cm^{-1} ($OCOO_2$) of CPMC was displaced towards 1330 cm^{-1} (Fig. 7 – 3, -5), whereas the one at 1588 cm^{-1} (NH_2) of Chit was moved to 1529 cm^{-1} (Fig. 7 – 2, -3, -4, -5). The lowering of the frequencies of the two bands confirmed the crosslinking of the chains of the two polymers by the association of these two groups (Fig. 7 – 5).

In contrast to the above-described results, we noticed that the characteristic band located at 886 cm^{-1} (P = O bond, elongation) of the TPP (Fig. 7 – 1), was shifted toward slightly higher wave numbers of the order of 892 cm^{-1} (Fig. 7 – 5), owing to the formation of the crosslinking bridge between the two polymer chains [43]. For Aml loaded into microspheres, the FT-IR analyses were performed in accordance with the chemical structure of Aml shown in Fig. 8.

The two bands at 1088 cm^{-1} and at 1113 cm^{-1}, respectively bonds of the sulfonium group -SO_3H and COC bonds of the ether functions [1], underwent an overlap and a shift toward a higher frequency at approximately 1144 cm^{-1} (Fig. 7 – 5, -6). In contrast, the two bands at 1262 cm^{-1} and

1200 cm^{-1} (elongation of C-N of the amine group) shifted to lower frequencies, at 1213 cm^{-1} and 1150 cm^{-1} respectively, although the 1300 cm^{-1} band shifted to higher frequencies, in the order of 1330 cm^{-1}.

We noticed the decrease in the frequency of the (-NH^+) bond (deformation vibration) of the protonated secondary amine of pyridinium (1491 cm^{-1}; Fig. 7 – 5), owing to its association with the oxygen of the carbonate group -(O-CO_2-) of CPMC (Fig. 7 – 3), through hydrogen bonds.
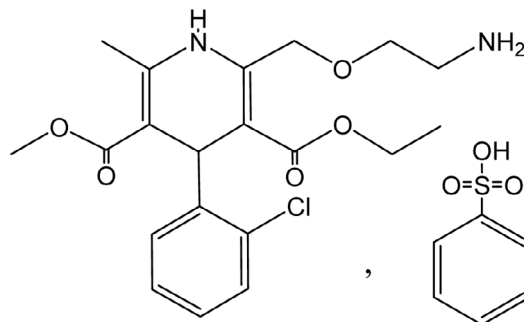

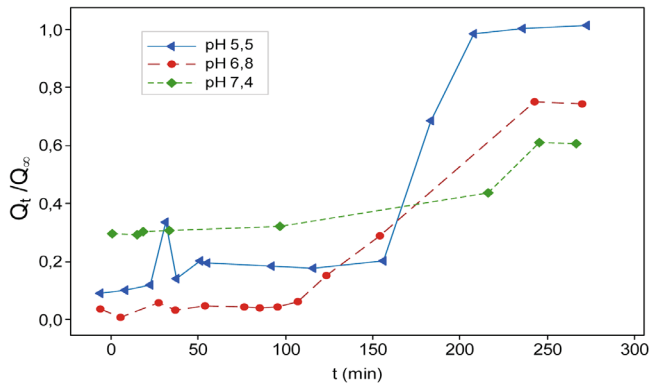**Fig. 8.** Chemical structure of amlodipine besylate.

Fig. 9. Amlodipine release kinetics curves from the FMP13 formulation in the three physiological media: duodenal (pH 5.5), intestinal (pH 6.8), and blood (pH 7.4). (All data given in mean ± SD, where SD = 1% is error percentage for the number of experiments = 3).
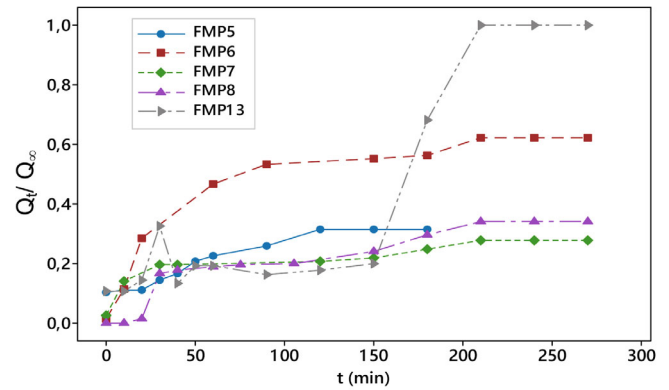

Fig. 10. Effects of formulation conditions on the release kinetics profiles of Aml in the duodenal medium. (All D-data given in mean ± SD, where SD = 1% is the error percentage for the number of experiments = 3).

Three bands, of CO (elongation of the two ester functions) at 1696 cm^{-1} and 1671 cm^{-1} and of NH$_2$ (deformation) of Aml, overlapped and shifted toward lower frequencies of the order of 1617 cm^{-1} (Fig. 7 – 5, -6), which interfered with the CO band (elongation) of Chit, located at a lower frequency in the microparticles (Fig. 7 – 5).

Furthermore, no band associated with Aml was observed on the spectrum of microparticles without an active ingredient. However, similar shifts in the characteristic bands of chitosan, CPMC, and TPP were observed, showing that there were crosslinks among the three species (Fig. 7 – 4).

Aml release kinetic study from microspheres

Drug release kinetics were plotted according to the mathematical models made by software programs. The zero-order (6), first-order (7), Higuchi (8), and Korsmeyer–Peppas models (9), corresponding to the four equations, were expressed in cumulative form, Q_t is the mass percentage of Aml as a function of t, and Q_∞ (the rate of the drug at saturation equilibrium at the end of release, which corresponds to the initial percentage in the formulation and tends toward 100%).

$$Q_t = k_0 t \text{ (zero order)} \tag{6}$$

$$\frac{Q_\infty - Q_t}{Q_\infty} = e^{-k_1 t} \text{ (first order)} \tag{7}$$

$$Q_t = k_H t^{\frac{1}{2}} > \text{(Higuchi)} \tag{8}$$

$$\frac{Q_t}{Q_\infty} = k t^n > \text{(Korsmeyer–Peppas),} \tag{9}$$

where, Q_t/Q_∞ is a fraction of drug release at time t, k_0, k_1, k_H, and k are the release rate constants, and n is the release exponent.

Influence of the pH of the physiological medium on the release kinetics

Figure 9 shows the effect of medium pH on the release kinetics of Aml. This one was markedly greater in the duodenal medium at pH 5.5 ($Q_t = 100\%$). It was relatively higher than that observed for the intestinal medium at pH 6.8 ($Q_t = 75.2\%$) and for the blood medium at pH 7.4 ($Q_t = 60.55\%$), and reached a plateau at 210 min for pH 5.5, and at 240 min for pH 6.8 and 7.4.

Furthermore, the burst effect was more significant in the medium at pH 5.5 (30.27%) than in the other two media. We also noted that the release of the active substance underwent a delayed effect up to 150 min, then the release was faster and was maximal after 210 min. The process further entered an equilibrium phase, forming a plateau from 210 min to 270 min. The same phenomenon was observed in the intestinal environment, but the delayed effect was decreased to 100 min, the time from which the release rate was faster and increased linearly up to 240 min and reached a plateau from this time to 270 min.

In contrast, the release into the blood medium was higher than in the two other media from the first moments up to 150 min. The release kinetics in the blood medium increased slowly from zero to 210 min, before being faster up to 250 min and reaching a plateau from 250 min to 270 min. This showed that the amount of Aml adsorbed on the surface of the microspheres diffused more rapidly within the physiological duodenal medium.
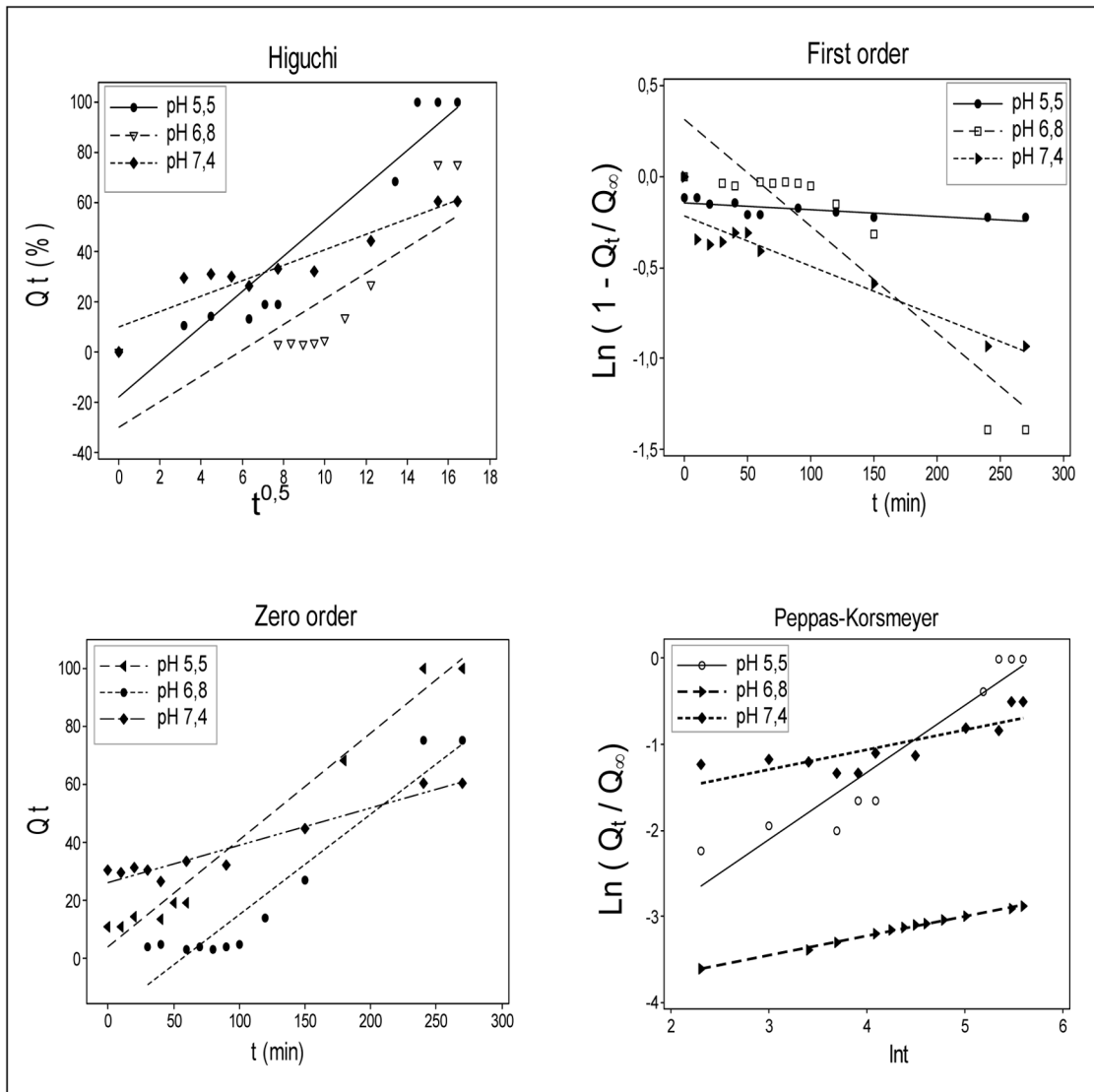
Fig. 11. Models of the release kinetics of amlodipine in different physiological media: duodenal (pH 5.5), intestinal (pH 6.8), and blood (pH 7.4). (All data given in mean ± SD, where SD = 1% is the error percentage for the number of experiments = 3).

Influence of formulation conditions on the release kinetics in the duodenal medium

In Fig. 10, we observe the variation of the release rate in the range 0 to 150 min, which is relatively faster and higher for FMP6 formulation (Q = 55.31%), whereas it was slower and lower for the other formulations (FMP5: 10.38%; FMP7: 27.72%; FMP8: 20% and FMP13: 20%).

Nevertheless, for times above 150 min, we noticed a marked increase in the speed and released quantity of Aml from FMP13 formulation (black circles), that reached the maximum release rate of 100% after 200 min of incubation. Aml release from FMP6 formulation reached a maximum of 62.19% after 210 min. For the three other formulations, FMP5 (31.55%), FMP7 (27.72%), and FMP8 (34.12%), the maximum levels reached were significantly lower.

Modeling of release kinetics

The results of the processing of the kinetics data showed that the pH of the physiological medium and the formulation conditions, by microencapsulation, significantly influenced the drug release mechanism from the formulations (Fig. 11).

This showed that for such microspheres, the release mechanism obeyed a transport process (Table 3), in accordance with the work of Unagolla and Jayasuriya [44], through a swelling matrix that disintegrated in a physiological medium of pH 5.5 close to the pH value of Chit dissolution (pH 5).

For the majority of formulations, we noticed that the value of n was less than 0.43 in the Korsmeyer–Peppas model, which was verified for at least three formulations,
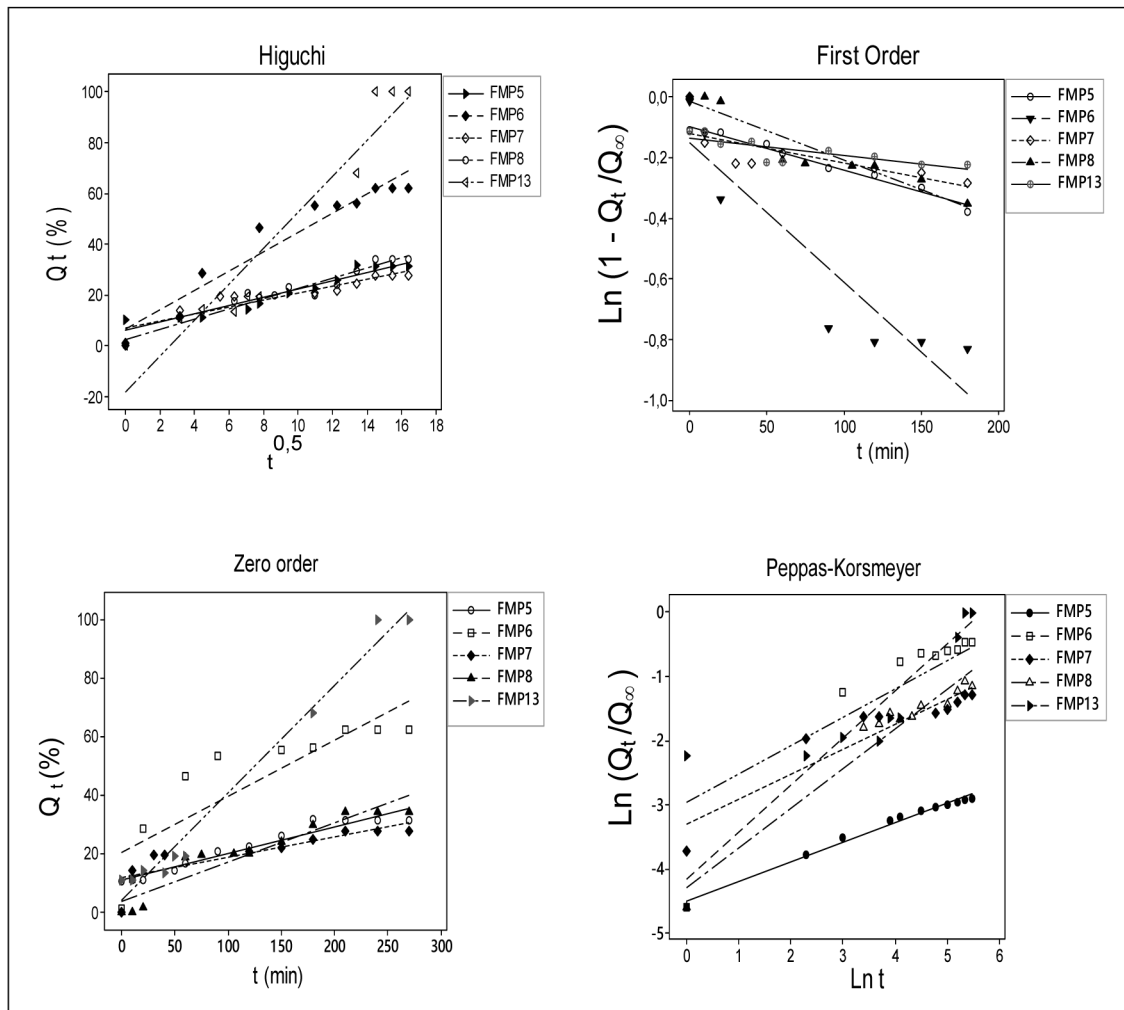
Fig. 12. Influence of the formulation conditions of chitosan/CPMC/amlodipine microspheres on the models of release kinetics in the duodenal medium. (All data given in mean ± SD, where SD = 1% is the error percentage for the number of experiments = 3).

FMP5 ($R^2 = 0.985$, $n = 0.265$), FMP7 ($R^2 = 0.986$, $n = 0.260$), and FMP13 ($R^2 = 0.993$, $n = 0.224$).

This means that the mechanism of the release kinetics obeyed much more a Fickian diffusion process. This transfer process occurs through a polydisperse polymer structure consisting of two layers and formed by the crosslinking of Chit and CPMC chains, as described in the work of Herdiana, et al. [45], except for FMP13 formulation (black circle) at pH 5.5 (duodenal), which had a value of $n = 0.78$, between 0.85 and 0.45.

Nevertheless, the model of order 1 (Fig. 12) seemed to be the least favorable, but it was only verified for FMP5 formulation ($X_1 = 1.125$, $X_2 = 4$, $X_3 = 4$), with a linear regression coefficient of the order of $R^2 = 0.985$ in duodenal medium (pH 5.5).

Moreover, it clearly appeared that the acidic pH of the TPP solution and of the polymers had a very great influence on the release mechanism of the drug, especially because it allowed a better rapprochement of the two polymer chains

(Chit and CPMC) and a hard crosslinking by protonation of the amino groups of Chit.

This caused the molecules of the active substance to diffuse through a more rigid matrix. On the other hand, the results showed that the Higuchi mechanism was more favorable at pH 5.5 ($R^2 = 0.936$) and 6.8 ($R^2 = 0.935$) for FMP13 formulation, owing to better diffusion of the medium within the microspheres, favored by the formation of micropores within the matrix.

In contrast to this, the first-order model seemed more favorable in the blood medium (pH 7.4) with an R^2 of around 0.954, where the matrix of FMP13 microspheres was more inert and less porous.

This agreed with the result obtained in the case of the Korsmeyer–Peppas model, which is not validated by the modeling results at pH 7.4 ($R^2 = 0.679$), for FMP13 formulation. At the same time, the zero-order model was favored in the duodenal medium at pH 5.5, for both FMP5 and FMP13 formulations.

TABLE 3. Models of the release kinetics of Aml from formulations in different physiological media

Formulation	pH	Kinetic Models								
		Higuchi		First Order		Zero order		Korsmeyer–Peppas		
		R^2	K_H	R^2	K_1	R^2	K_0	R^2	K	n
FMP5	5.5	0.967	0.0515	0.985	0.0012	0.983	0.1106	0.985	0.0077	0.265
FMP6	5.5	0.928	3.7968	0.864	0.0038	0.751	0.1930	0.928	0.0702	0,288
FMP7	5.5	0.898	0.9397	0.897	0.0006	0.841	0.0501	0.986	0.0081	0.260
FMP8	5.5	0.923	2.0372	0.915	0.0018	0.906	0.1599	0.909	0.0432	0.345
FMP13	5.5	0.936	7.9056	0.593	0.0006	0.981	0.3668	0.904	0.0044	0.780
FMP13	6.8	0.935	9.5046	0.882	0.0065	0.911	0.3452	0.993	0.0132	0.224
FMP13	7.4	0.874	2.5956	0.954	0.0025	0.938	0.1280	0.679	0.0714	0.230

It depended on the formulation conditions (TPP rate, pH of the TPP solution, pH of the polymer solution) of the experimental design. The mean value of the quantity of TPP ($X_1 = 1.125$ %) and the acidic pH of the polymer solution ($X_3 = 4$; 6) seemed to be the best conditions for this model. The release depended a lot on time and took place with the same quantity and at a relatively constant speed when the crosslinking existing between the chains of the two polymers was optimal.

CONCLUSION

Amlodipine-loaded microparticles were prepared by combining two polymers, Chit and CPMC, using TPP as a crosslinking agent. The process was optimized by a three-variable, three-level Box–Behnken experiment design. The formulation conditions of the microparticles significantly affected the optimized responses. According to the statistical study, the models obtained for the responses were significant, for the zeta potential and the encapsulation efficiency, and even much lower for the microparticle size. This response, for which the model was the most predicted, with a maximum R^2 regression coefficient, was influenced by the three factors: the quantity of TPP, the pH of the solutions of TPP, and the mixture of polymers. The zeta potential values were positive for all the formulations, and the particle size of the microparticles prepared met the standard required for drugs (sizes ≤ 10 μm) intended for the oral route with a low PDI value and a very high encapsulation efficiency.

Analyses by DSC, XRD, and FT-IR showed that the process of crosslinking the two polyelectrolytes led to changes in the structure of the polymers in the microparticles, which became more amorphous, promoting better dispersion of the active drug molecules in the matrix. The kinetics study allowed the correlation between the parameters of the encapsulation and the medium of the drug release. They both influenced the mechanism and the model of release. The latter was markedly higher and faster in the duodenal medium. The mechanism took place according to the zero-order model,

promoting prolonged release. In addition, the Aml release was slower with a lower rate, according to the Korsmeyer–Peppas model in the intestinal medium. However, when varying the conditions of the encapsulation, the first-order and Higuchi models were favored in the duodenal medium, which is the best target site of absorption for this drug.

Disclosure of interest

The authors report no conflicts of interest.

REFERENCES

1. T. Niaz, S. Shabbir, S. Manzoor, et al., *Carbohydr. Polym.*, **142**, 268 – 274 (2016).
2. M. R. Badwar, S. L. Borse, M. S. Junagade, et al., *Int. J. App. Pharm.*, 132 – 139 (2019).
3. M. S. Kaynak, A. Bogacz, M. Stelmasinski, et al., *FABAD J. Pharma. Sci.*, **36**(4), 207 – 222 (2011).
4. N. Swamy and Z. Abbas, *Ind. J. Pharma. Sci.*, **73**(6), 608 – 614 (2011).
5. M. G. Antoniraj, M. M. Leena, J. Moses, et al., *Int. J. Biol. Macrom.*, **147**, 1268 – 1277 (2020).
6. R. Sari, M. Galda, W. Lestari, et al., *Asian J. Pharm. Clin. Res.*, **8**(1), 331 – 333 (2015).
7. L. S. Guinesi and É. T. G. Cavalheiro, *Thermochim. Acta*, **444**(2), 128 – 133 (2006).
8. E. M. Hejjaji, A. M. Smith, G. A. Morris, *Int. J. Biol. Macromol.*, **120**, 1610 – 1617 (2018).
9. R. Riva, H. Ragelle, A. des Rieux, et al., *Adv. Polym. Sci.*, **244**(1), 19 – 44 (2011).
10. O. U. Akakuru, H. Louis, P. I. Amos, et al., *Biochem. Pharmacol. (Los Angel.)*, **7**(1), 1000241 (2018).

11. R. Arévalo-Pérez, C. Maderuelo, J. M. Lanao, *J. Control. Release*, **327**, 703 – 724 (2020).

12. D. Kida, A. Zakrzewska, J. Zborowski, et al., *Materials*, **14**(14), 3948 (2021).

13. G. Cavallaro, S. Micciulla, L. Chiappisi, et al., *J. Mater. Chem. B*, **9**(3), 594 – 611 (2021).

14. L. Zhou, H. Shi, Z. Li, et al., *Macromol. Rapid Commun.*, **41**(21), 2000149 (2020).

15. Z. Li and Z. Lin, *Aggregate*, **2**(2), e21 (2021).

16. N. K. Al-Nemrawi, S. S. M. Alsharif, R. H. Dave, *Int. J. Appl. Pharm.*, **10**, 60 – 65 (2018).

17. G. Vozza, M. Danish, H. J. Byrne, et al., *Int. J. Pharm.*, **551**(1 – 2), 257 – 269 (2018).

18. S. Bouriche, M. J. Cózar-Bernal, F. Rezgui, et al., *J. Drug Deliv. Sci. Technol.*, **51**, 419 – 429 (2019).

19. K. M. Mostafa and A. El-Sanabary, *J. Appl. Polym. Sci.*, **88**, 959 – 965 (2003).

20. J. O. Akolade, H. O. B. Oloyede, M. O. Salawu, et al., *J. Drug Deliv. Sci. Technol.*, **4**, 1 – 31 (2018).

21. G. R. Chatwal and S. K. Anand, *Instrumental methods of chemical analysis*, 5th ed., Himalaya Publishing House (2009), pp. 249 – 251.

22. L. Zhao, B. Zhu, Y. Jia, et al., *Biomed. Res. Int.*, 1 – 7 (2013).

23. S. Bindhani, S. Mohapatra, R. Kar, *Int. J. App. Pharm.*, **12**(2), 94 – 102 (2020).

24. N. K. Al-Nemrawi, S. S. M. Alsharif, R. H. Dave, *Int. J. App. Pharm.*, **10**(5), 60 – 65 (2018).

25. M. J. Martin, A. C. Calpena, F. Fernandez, et al., *Carbohydr. Polym.*, **117**, 140 – 149 (2015).

26. I. J. Joye and D. J. McClements, *Curr. Opin. Colloid Interface Sci.*, **19**(5), 417 – 427 (2014).

27. F. Zhang, X. Cai, L. Ding, *Food Hydrocoll.*, **111**, 106211(2021).

28. K. Desai and H. J. Park, *J. Microencapsul.*, **23**(1), 91 – 103 (2006).

29. C. Y. Yang, C. H. Hsu, M. L. Tsai, *Carbohydr. Polym.*, **86**(2), 659 – 665 (2011).

30. J. M. Rabanel, V. Adibnia, S. F. Tehrani, et al., *Nanoscale*, **11**(2), 383 – 406 (2019).

31. Z. Du, J. Liu, T. Zhang, et al., *Food Chem.*, **286**, 530 – 536 (2019).

32. S. Hassani, A. Laouini, H. Fessi, et al., *Colloids Surf. A. Physicochem. Eng. Asp.*, **482**, 34 – 43 (2015).

33. S. Kunjachan, S. Jose, T. Lammers, *Asian J. Pharm.*, **4**(2), 148 – 153 (2014).

34. A. Moeini, A. Cimmino, G. Dal Poggetto, et al., *Carbohydr. Polym.*, **195**, 631 – 641 (2018).

35. G. Thandapani, S. Prasad, P. Sudha, et al., *Int. J. Biol. Macromol.*, **104**, 1794 – 1806 (2017).

36. Z. Sang, J. Qian, J. Han, et al., *Carbohydr. Polym.*, **230**, 115577 (2020).

37. R. C. Dhakar, S. D. Maurya, V. Saluja, *J. Drug Deliv. Ther.*, **2**(6), 128 – 133 (2012).

38. A. J. Ribeiro, C. Silva, D. Ferreira, et al., *Eur. J. Pharm. Sci.*, **25**(1), 31 – 40 (2005).

39. H. Abd-Allah, A. O. Kamel, O. A. Sammour, *Carbohydr. Polym.*, **149**, 263 – 273 (2016).

40. S. S. Patil, V. Mohan Gupta, S. Gupta, et al., *J. Biomed. Pharm. Res.*, **3**(3), 51 – 58 (2014).

41. A. Kalia, S. Khurana, N. Bedi, *Int. J. Pharm. Pharm. Sci.*, **1**(1), 12 – 23 (2009).

42. M. Motiei and S. Kashanian, *Eur. J. Pharm. Sci.*, **99**, 285 – 291 (2017).

43. E. C. Sekhar, K. K. Rao, R. R. Raju, *J. App. Pharm. Sci.*, **1**(8), 199 – 204 (2011).

44. J. M. Unagolla and A. C. Jayasuriya, *Eur. J. Pharm. Sci.*, **114**, 199 – 209 (2018).

45. Y. Herdiana, N. Wathoni, S. Shamsuddin, et al., *Heliyon*, **8**, e08674 (2022).